BEHAVIOR OF MULTIPLE BROADBAND GROUND MOTION SIMULATION TECHNIQUES FOR A SUITE OF EARTHQUAKE SCENARIOS USING MULTIPLE RUPTURE MODEL GENERATORS ON THE SCEC BROADBAND PLATFORM

2012 SCEC Project Report (Award #12098)

Jeff Bayless, URS
Dr. Paul Somerville, URS

Abstract

Simulations were performed on the SCEC Broadband Platform for a suite of earthquake scenarios, using multiple rupture generators (GP and UCSB) and three broadband simulation techniques (GP, UCSB, SDSU). RotD50 was computed at 60 total sites in 20 and 40 kilometer distance-to-rupture bands around the fault plane for each scenario/rupture generator/simulation technique combination, using the default parametric settings for each technique. The spectral amplitude predictions were compared between each simulation technique over the period range of 0.01-10 seconds in order to provide insight as to how the methods, in their default form, compare given the same input rupture model. These insights will serve as a baseline for referencing the future differences observed between models; a) when default settings are adjusted and b) for forward earthquake validations and simulations, to allow for meaningful comparisons. In addition to analyzing the average results with respect to spectral period, spatial comparison results are presented in map form – both to compare simulation techniques with each other, and to compare simulation predictions with those of several Ground Motion Prediction Equations. Results are presented for the first earthquake scenario, using both rupture generators. Further interpretation of the results not presented here will be documented in a supplemental report to SCEC, utilizing finalized versions of the Broadband Platform simulation codes.

Table of Contents

1. Introduction

1.1 The SCEC Broadband Ground Motion Simulation Platform

The SCEC Broadband Ground Motion Simulation Platform (BBP) has become an important resource for researchers and practitioners who need to use strong ground motion simulations. The BBP allows a user (who need not be the developer of any simulation procedure) to generate ground motions for a particular earthquake scenario using modular physics-based simulation methods. The BBP provides the user with the flexibility to select from various alternative approaches for generating the earthquake rupture description, modeling low- and high-frequency wave propagation, and incorporating site effects. These different components of the simulation are assembled in modules which can be combined to run in multiple permutations, producing broadband seismograms. The Platform is part of the SCEC Community Modeling Environment in which SCEC scientists collaborate in the construction of shared data bases and computational platforms. Three sets of simulation procedures have already been installed on the BBP and are utilized in this project:

- GP (Graves and Pitarka, 2010)
- UCSB (Schmedes et al., 2010, 2011; Liu, 2006)
- SDSU-ETH (Mai et al., 2010; Mena et al., 2010)

1.2 Objectives of this Project

In previous BBP related projects, comparisons were made between simulations and recordings for each modeling technique, but rigorous comparisons between the results of the different modeling techniques were not made (Bayless et al., 2011). We address the observation made by Norm Abrahamson that when the three modeling groups are asked to reproduce the ground motions of a past earthquake, the three simulation techniques tend to be in agreement with each other, but when asked to simulate a future earthquake scenario, results vary considerably. This situation is hindering acceptance of the Broadband Platform for use in strong ground motion simulations.

The main objectives of this project are to:

- Analyze the behavior of the three broadband simulation methods currently on the SCEC Broadband Platform with their default settings for a suite of scenario earthquake events with varying magnitude. Predicted ground motions will be compared between the simulation techniques over a range of frequencies and recording distances.
- Analyze each scenario event for both rupture generator methods currently on the SCEC Broadband Platform (GP and UCSB).
- Provide insight as to how the methods, in their most basic, default form, compare given the same input rupture model. Demonstrate the performance of each simulation technique relative to the other methods. These insights will serve as a baseline for referencing the future differences observed between models; a) when default settings are adjusted and b) for forward earthquake validations and simulations.

2. Methodology

2.1 Earthquake Scenarios and Rupture Models

This work utilizes a suite of earthquake scenarios developed by the Southwestern U.S. (SWUS) Ground Motion Characterization (GMC) simulation validation project through SCEC; in particular Part B: validation of simulation methods with ground motion prediction equations (GMPEs). Coordinating earthquake scenarios with this project will allow for meaningful comparisons as the simulation techniques go through the validation process, and also encompasses a range of earthquakes for which the simulation techniques are well-constrained. These six scenarios and their properties are listed in Table 1. For each scenario both the GP and UCSB rupture generators were used to generate two alternative rupture models, leading to 12 total rupture models for the 6 scenarios.

Table 1. Earthquake scenarios used for developing scenario rupture models.

Scenario Name	Mechanism	Region (Velocity Model)	Mw	L (km)	W (km)	Ztor (km)	Strike (deg)	Rake (deg)	Dip (deg)
EQ1	Strike-Slip	So-Cal	6.2	17.8	8.9	4.0	0	180	90
EQ2	Strike-Slip	Nor-Cal	6.2	17.8	8.9	4.0	0	180	90
EQ3	Reverse	So-Cal	6.6	28.2	14.1	3.0	0	90	45
EQ4	Reverse	Nor-Cal	6.6	28.2	14.1	3.0	0	90	45
EQ5	Strike-Slip	So-Cal	6.6	28.2	14.1	0.0	0	180	90
EQ6	Strike-Slip	Nor-Cal	6.6	28.2	14.1	0.0	0	180	90

2.2 Simulations on the BBP

For each scenario and rupture model generator we used the GP, UCSB and SDSU-ETH broadband simulation methods on the SCEC Broadband Platform (see Figure 1) with their default parameter settings. For the northern California scenarios the “LOMAP” (Loma Prieta) velocity model and Green’s functions are used. For the southern California scenarios the “LABasin” velocity model and Green’s functions are used. These distinctions are also in line with the SWUS GMC validation project. Site effects modules were not incorporated in the simulations, so all synthetics are performed for “rock” site conditions.

At the time of writing, UCSB Green’s functions for the southern and northern California regions were not completed for use on the BBP, and so the available “Northridge” Green’s functions were used in the southern California simulations as a placeholder. Additionally, through close interaction with the UCSB and SDSU code developers, we have learned that current code versions on the BBP are not finalized (as of March 2013) and require updates. Current work on this portion of the project is aimed at coordinating with UCSB, SDSU and SCEC IT to complete the UCSB module compatibility and update all code to their final versions.

2.3 Analysis of Results and Deliverables

Upon completion of scenario simulations performed on the BBP, the product is a pair of two-component acceleration seismograms at each site, from which the Rotd50 component of 5% damped pseudo-spectral acceleration (Sa) is calculated over the range of 0.1-100 Hz. Results comparing the different

techniques are presented as "Ratio" plots for each scenario event. The Ratio plots represent the natural log of the ratio of RotD50 spectral acceleration at a given period (*T*) calculated from one simulation technique (*j*) relative to another (*k*), averaged over all recording stations (*i*):

$$Ratio(T,j,k) = \frac{1}{N}\sum_{N}^{i=1} ln\left(\frac{Sa(T)_{i,j}}{Sa(T)_{i,k}}\right); \quad (1)$$

This process was repeated to compare simulation techniques GP, UCSB, and SDSU-ETH, and the results are presented as Ratio plots versus period showing the mean value over all sites, 90% confidence interval, and the mean plus or minus one standard deviation (Figure 4).

In addition to Ratio plots versus period, maps of the Ratio at each simulation site are produced for various response spectral periods, including PGA (Figure 5, left column). On the same figures (right column) we illustrate maps of validation with spectral acceleration predicted by the average of the four 2008 Next Generation Attenuation (NGA) GMPE's (Abrahamson et al., 2008), calculated for reference site conditions, for a given simulation method. The Ratio maps allow for analysis of the relative performance of the simulation techniques in space for a specific period of interest, and the GMPE maps provide a reference point for these comparisons. The predictions resulting from the two different rupture model generators are presented separately and can be compared side by side.

3. Results and Discussion

3.1 Earthquake Scenario EQ1 (M6.2 Strike-Slip)

The results of BBP simulations for EQ1 show that the different techniques in their default form used for an Mw 6.2 strike-slip event in southern California obtain vastly differing RotD50 predictions on average. Figure 4 shows the Ratio plot with spectral period for the GP rupture of EQ1. In the top panel is the GP/UCSB Ratio, the middle panel the UCSB/SDSU Ratio, and the bottom panel the SDSU/GP (this format is consistent for all subsequent figures.) All three Ratios show relatively good agreement at longer periods, specifically at T > 1.0s. The GP technique predicts larger spectral values from UCSB by a factor not exceeding 2 (Ratio =0.75) in this period range. As expected, the GP/SDSU comparison shows a Ratio of unity at long periods, which is expected because both methods use the same deterministic formulation (Mai et al., 2010; Mena et al., 2010; Graves and Pitarka, 2010). At shorter periods (T < 1.0s), where GP uses a stochastic formulation, a wide range of variation is observed. Relative to the UCSB method, GP predicts larger spectral values, and the magnitude of the difference is greatest between 0.1 and 1.0 seconds. Relative to the SDSU method, GP predicts larger spectral values as well, but to a slightly lesser degree. At PGA the maximum mean Ratio for the GP/UCSB comparison is roughly Ratio =1.6, meaning nearly a factor of 5 difference between the two. For SDSU/GP at PGA the mean Ratio is closer to Ratio =1.0, about a factor of 2.7 different.

Figures 5 and 6 show maps of the spatial Ratio for individual stations at PGA and Sa at T=1.0s, respectively, for the GP rupture of EQ1. In these figures "warm" colors represent positive residuals or larger predictions, and "cool" colors represent negative residuals or smaller predictions. Working from the top row down, the right column maps represent the GP, UCSB, and SDSU residuals from the average predictions of the four 2008 NGA GMPE's (hereafter referred to as the "NGA"). In Figure 5 (PGA) GP shows excellent agreement with the NGA at nearly every site, both for the 20 and 40 km tracks of sites around the fault. The dark red larger-predictions of the GP/UCSB comparison can be observed on the

top row, as well as the corresponding dark blue under-prediction of the UCSB simulations relative to the NGA (middle row, right column). UCSB predictions show a tendency to predict more closely matching RotD50 to SDSU in the 20km track than the 40km track (middle row, left column). SDSU shows a somewhat consistent underprediction to the NGA (right column, bottom row) for all sites, and a similar relationship to the GP method at all sites.

In Figure 6 (Sa at 1.0s) less of the deep blue and red markers are observed, meaning relatively smaller differences between simulation techniques. Generally the trends of Ratios and residuals in space are similar at PGA (Figure 5), except less distinguished at 1.0s. GP again shows good agreement with the NGA, and a prediction of higher RotD50 than the UCSB method, more strongly so on the 40km track. This higher prediction is notably weakest in the southern portions of the map, along strike of the fault. The UCSB method again under-predicts relative to the NGA (middle row, right column), but to a much lesser degree than at PGA. Again the under-prediction appears weaker on the 20km track and the southern region, and UCSB predictions show a tendency to predict more closely matching RotD50 to SDSU in the 20km track than the 40km track. Relative to GP and the NGA, SDSU tends to under-predict RotD50 except at sites along strike of the fault, at both ends of the 40km track. This is perhaps the influence of directivity already appearing in the SDSU method, which is not accounted for directly in the NGA.

Now that the similarities and differences of the simulation methods given the same input rupture model have been discussed, we provide commentary on an individual technique's sensitivity to the two rupture models. Figures 4 and 7 compare the sets of Ratio for the EQ1 scenario using the GP and UCSB rupture generators, respectively. The UCSB/SDSU mean Ratio (middle panels) have similar shape and values across the entire frequency range, meaning the RotD50 predictions of these two techniques are not highly dependent of the rupture generator used for this simulation. The GP method, however, shows stronger over-prediction relative to UCSB and SDSU at T <1.0s for the UCSB rupture generator. The overall shape of the mean GP/UCSB and SDSU/GP Ratio plots are similar for the two rupture generators, meaning the two different generators do not yield drastically different results to the point that the Ratio is inverted. In short, the mean Ratio shapes for all of the simulation technique comparisons are similar but the differences between techniques are slightly more extreme for the UCSB rupture generator at periods less than one second.

To compare the spatial predictions of the simulation techniques and their sensitivity to rupture generator, let us first consider the PGA maps plotted in Figure 8 (UCSB rupture generator), compared with the results discussed previously in Figure 5 (GP rupture generator). For the GMPE comparison, the GP method is less than 0.5 log units of residuals for all stations, but the most striking feature of Figure 8 (UCSB rupture) is the difference in the northern and southern portions. The sites to the north of the hypocenter tend to over-predict the NGA GMPEs, while sites to the south tend to under-predict. This is likely due to the imbalance of slip along strike observed in the UCSB rupture for EQ1 (Figure 3). This figure clearly shows increased levels of slip in the northern portion of the fault (right side in the figure since strike is zero degrees). In Figure 8, this phenomenon is not observed for the other simulation techniques, nor for any of the techniques using the GP rupture generator (Figure 5). As the mean Ratio comparison suggests, at PGA the simulation technique comparison maps otherwise behave similarly when comparing between rupture model generators.

Figures 9 and 6 compare the simulation techniques' sensitivity to rupture generator at one second period. In Figure 9, for the GP simulation compared with the NGA GMPEs, the strong dependence on location along the fault observed at PGA is not present. However, for both the UCSB and SDSU

technique, the simulations tend to predict larger RotD50 at both ends of the fault (along strike) for the UCSB rupture method than the GP rupture method. This is only observed in cases with small source to site azimuth.

3.2 Scenarios EQ2 – EQ6

Further interpretation of the results not presented here will be documented in a supplemental report to be submitted to SCEC in the fall of 2013, and as a presentation at the 2013 SSA Annual Meeting. Additionally, as the UCSB and SDSU codes and Green's Functions are finalized and frozen on the BBP, these results will be updated.

4. References

Abrahamson N.A. et al. (2008), Comparisons of the NGA ground motion relations. Earthquake Spectra 24, 45-66.

Bayless, J., A. Pitarka, S. Ni and P. Somerville (2011). Validation of broadband strong motion simulations for the NGA East Project – summary of results. http://peer.berkeley.edu/ngaeast/wp-content/uploads/2011/10/Th_AM_3_Bayless-Somerville_URS-Validation-Results.pdf

Graves, R.W. and A. Pitarka (2010). Broadband Ground-Motion Simulation Using a Hybrid Approach, Bull. Seism. Soc. Am., Vol. 100, No. 5A, pp. 2095-2123, doi:10.1785/0120100057

Liu, P., R. J. Archuleta and S. H. Hartzell (2006). Prediction of broadband ground-motion time histories: Hybrid low/high-frequency method with correlated random source parameters, Bull. Seismol. Soc. Am. vol. 96, No. 6, pp. 2118-2130, doi: 10.1785/0120060036.

Mai, P.M., W. Imperatori, and K.B. Olsen (2010). Hybrid broadband ground-motion simulations: combining long-period deterministic synthetics with high-frequency multiple S-to-S back-scattering, Bull. Seis. Soc. Am.. 100, 5A, 2124-2142.

Mena, B., P.M. Mai, K.B. Olsen, M.D. Purvance, and J.N. Brune (2010). Hybrid broadband ground motion simulation using scattering Green's functions: application to large magnitude events, Bull. Seis. Soc. Am. 100, 5A, 2143-2162.

Schmedes, J., R. J. Archuleta, and D. Lavallée (2010). Correlation of earthquake source parameters inferred from dynamic rupture simulations, J. Geophys. Res., 115, B03304, doi:10.1029/2009JB006689.

Schmedes, J., R. J. Archuleta, and D. Lavallée (2011). A kinematic rupture model generator incorporating spatial interdependency of earthquake source parameters, to be submitted to Journal of Geophysical Research.

5. Figures

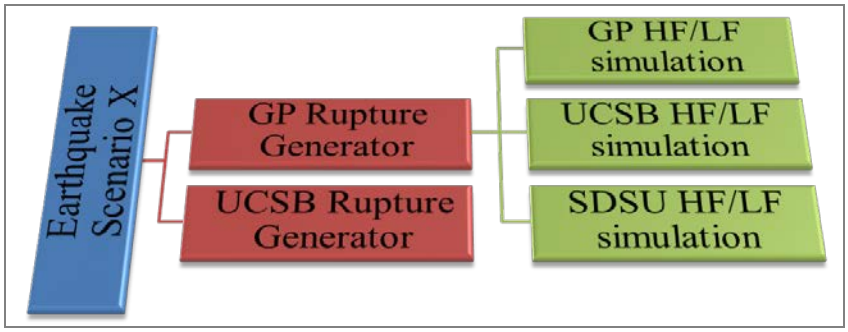

Figure 1. Hierarchy tree for broadband simulations, one earthquake scenario.

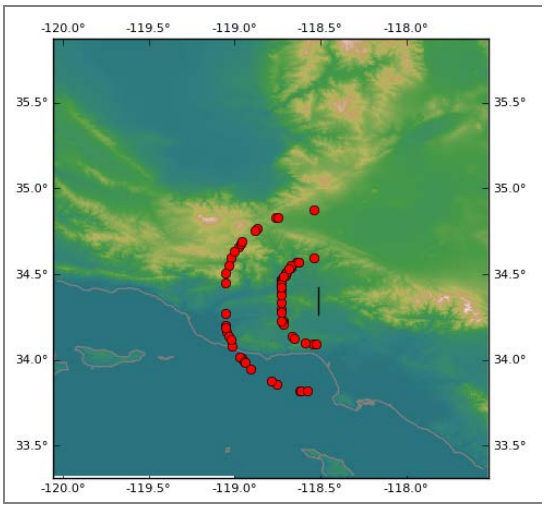

Figure 2. Map of the EQ1 fault scenario (black line) and surrounding simulation sites (red circles). Simulation locations are two half "racetracks" of 30 sites each around the fault at Rrup of 20 and 40 km, selected randomly from a set of closely spaced sites. Color shadings show topography and do not effect simulations, which are all done for rock site conditions.

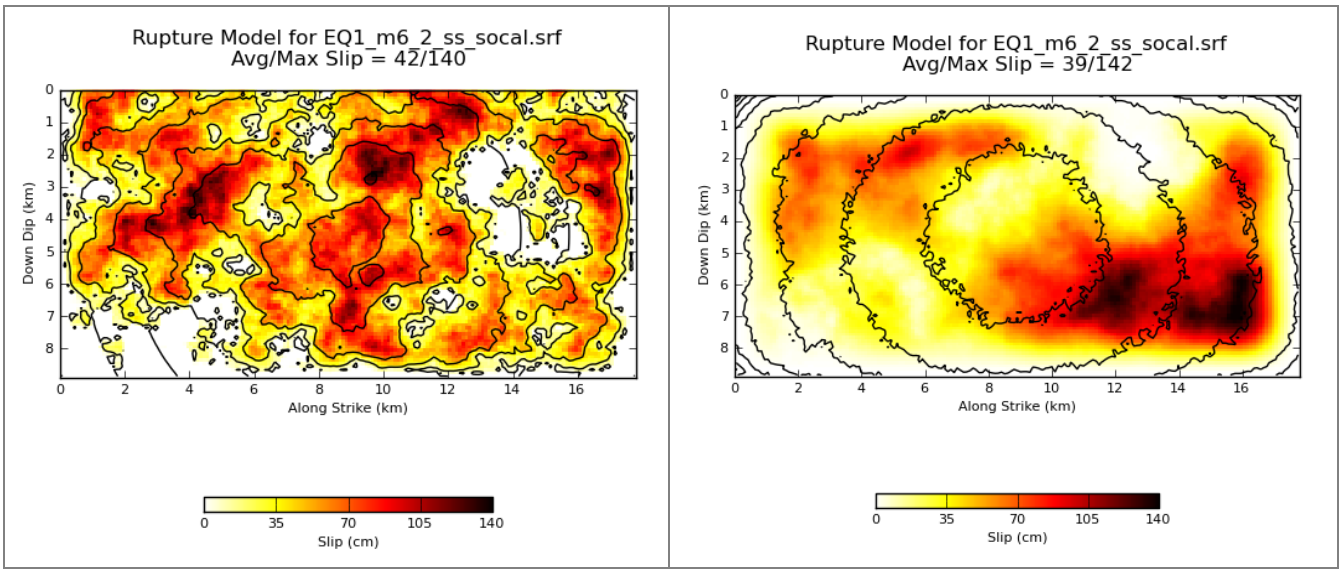

Figure 3. Plot of the EQ1 rupture models using the GP (left) and UCSB (right) rupture generators.

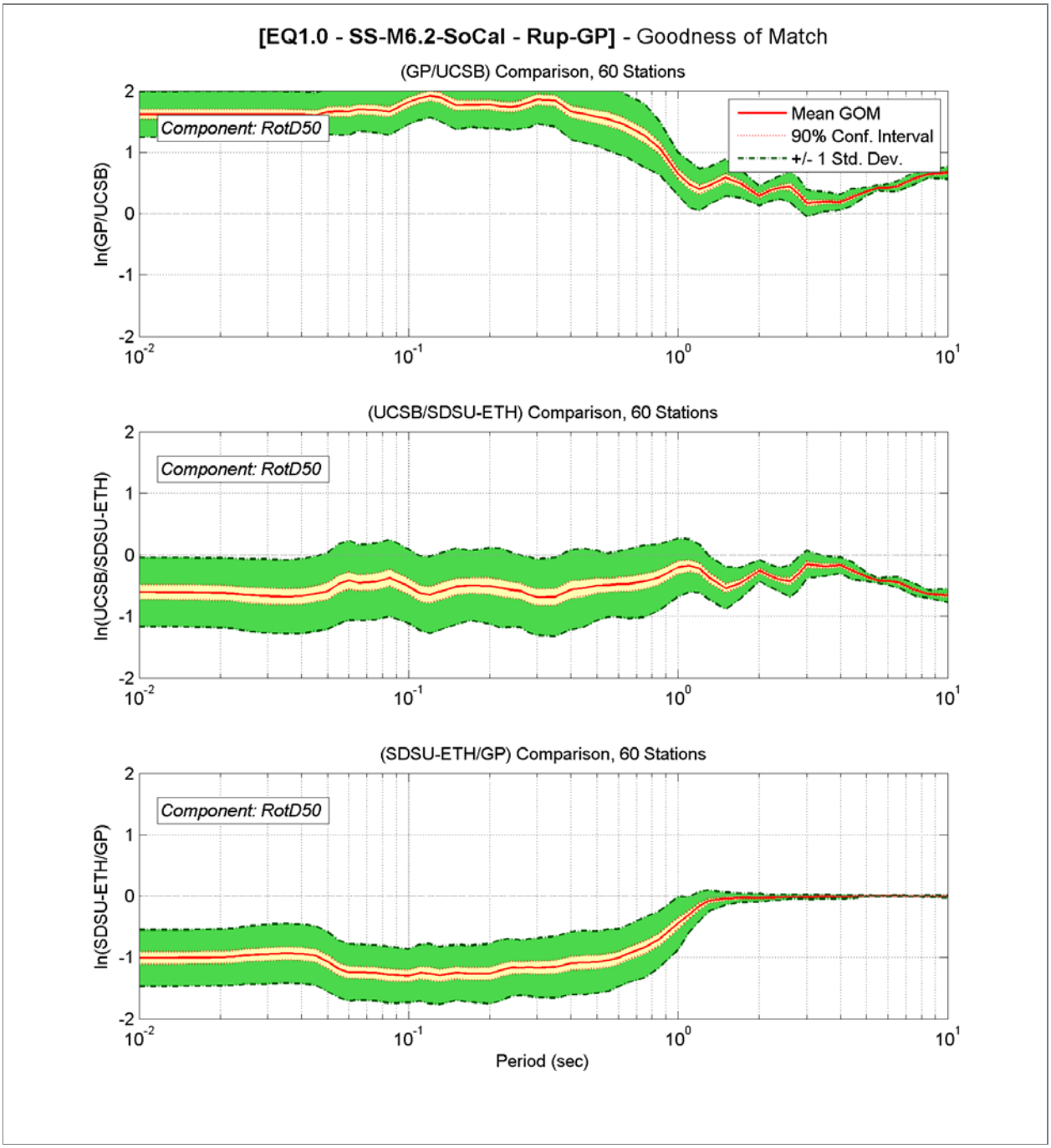

Figure 4. Ratio plots for EQ1 (GP rupture model) comparing RotD50 response spectral accelerations at varying periods calculated from one technique relative to another. Top panel: GP/UCSB. Middle panel: UCSB/SDSU. Bottom panel: SDSU/GP. The red line represents the mean ratio of all recording stations, and the yellow and green shaded areas represent the 90% confidence interval and mean +/- 1 standard deviation, respectively.

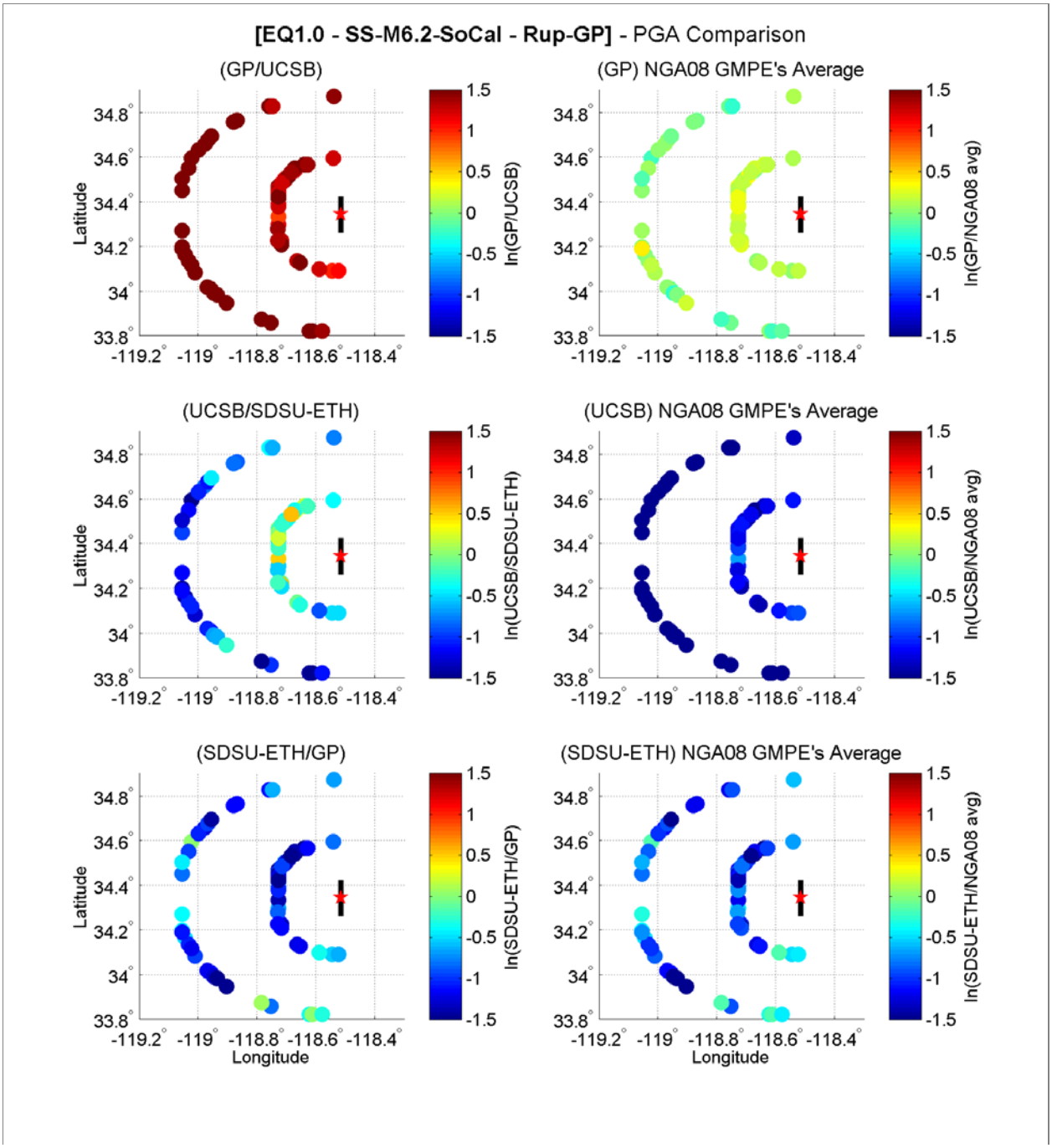

Figure 5. Maps of spatial Ratios (left column) and NGA residuals (right column), PGA, for EQ1 (GP rupture). Top row: GP/UCSB. Middle row: UCSB/SDSU. Bottom row: SDSU/GP.

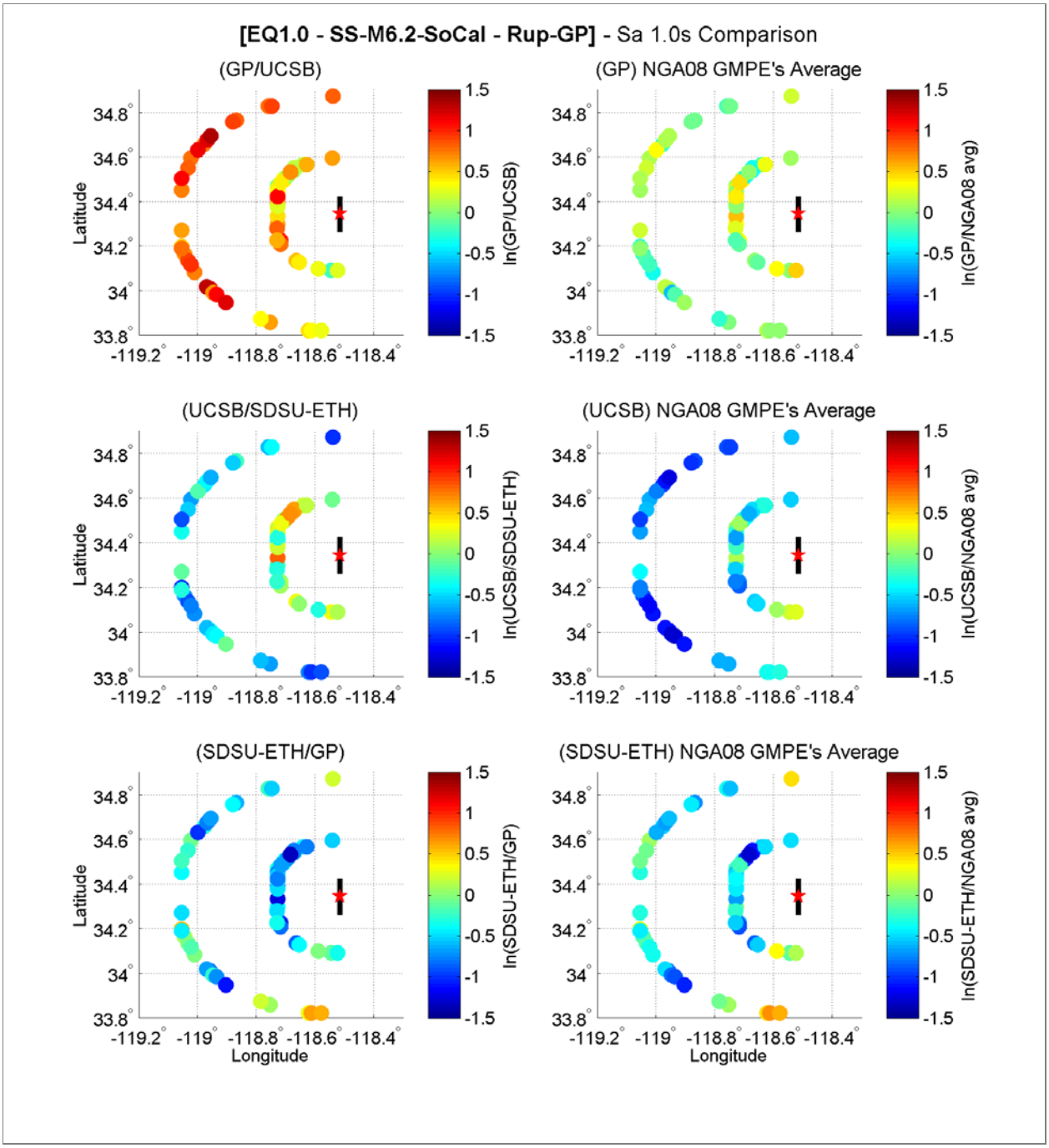

Figure 6. Maps of spatial Ratios (left column) and NGA residuals (right column) , Sa at 1.0 seconds, for EQ1 (GP rupture). Top row: GP/UCSB. Middle row: UCSB/SDSU. Bottom row: SDSU/GP.

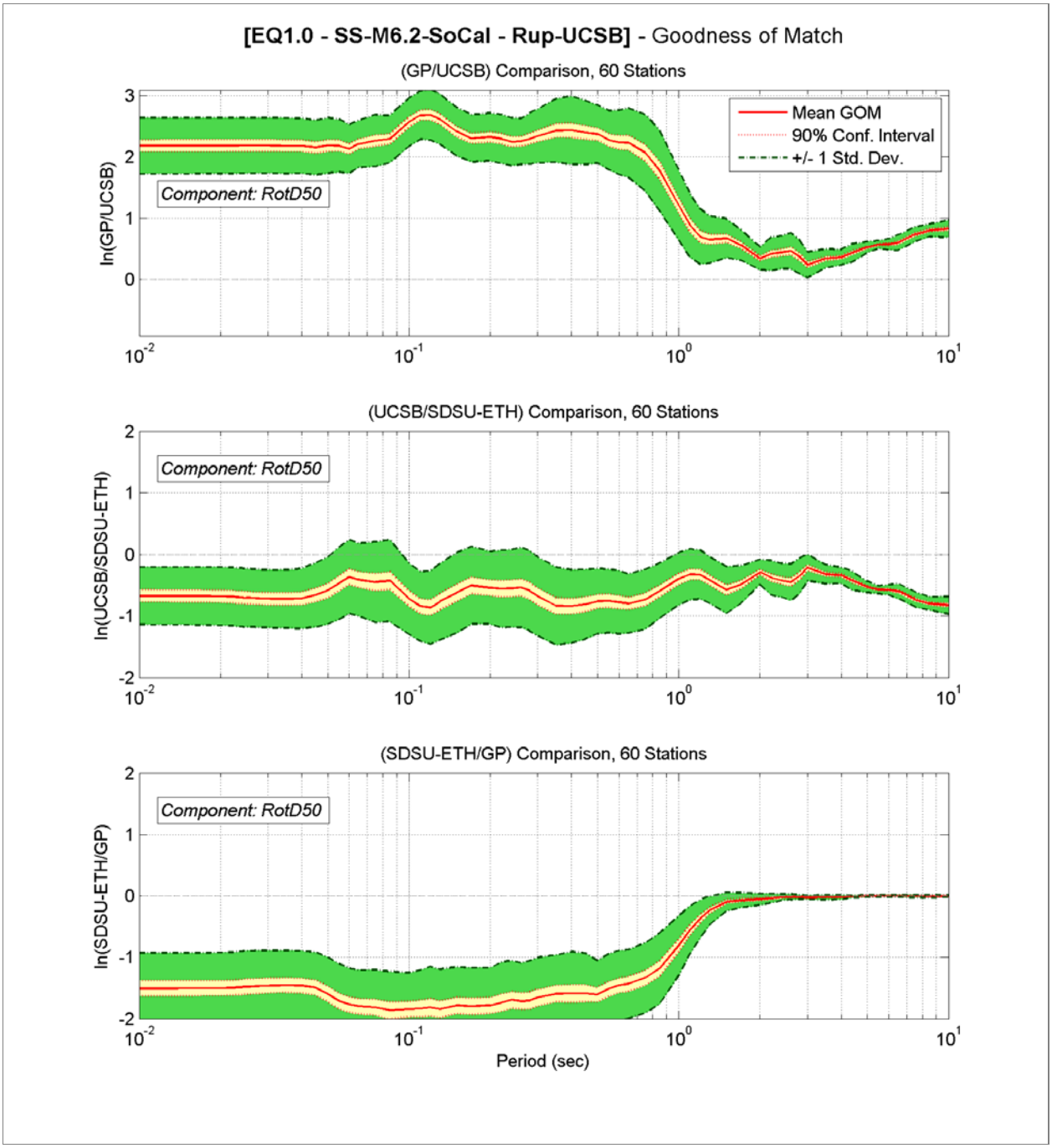

Figure 7. Ratio plots for EQ1 (UCSB rupture model) comparing RotD50 response spectral accelerations at varying periods calculated from one technique relative to another. Top panel: GP/UCSB. Middle panel: UCSB/SDSU. Bottom panel: SDSU/GP. The red line represents the mean ratio of all recording stations, and the yellow and green shaded areas represent the 90% confidence interval and mean +/- 1 standard deviation, respectively.

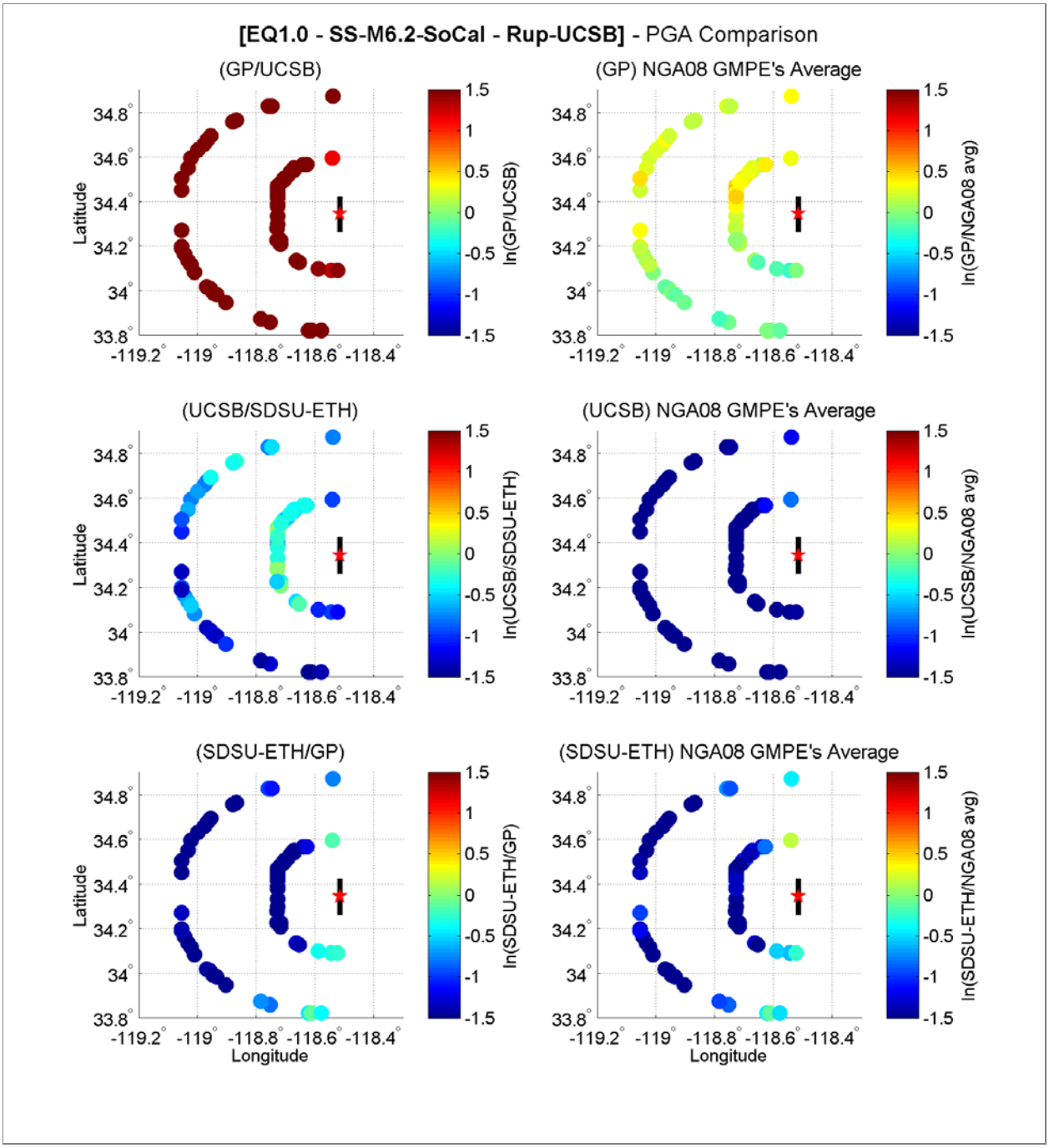

Figure 8. Maps of spatial Ratios (left column) and residuals (right column), PGA, for EQ1 (UCSB rupture). Top row: GP/UCSB. Middle row: UCSB/SDSU. Bottom row: SDSU/GP.

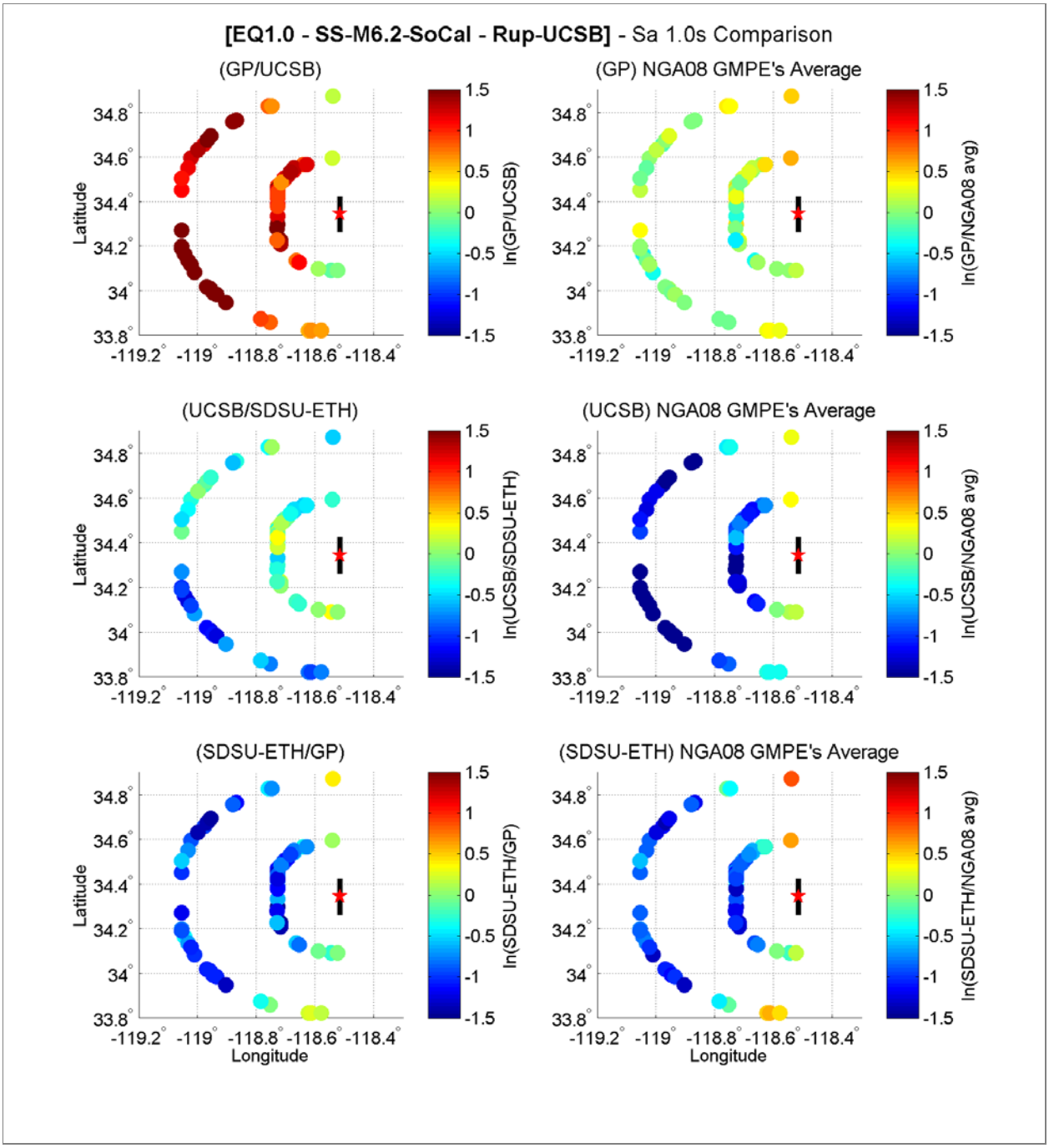

Figure 9. Maps of spatial Ratios (left column) and residuals (right column), Sa at 1.0 seconds, for EQ1 (UCSB rupture). Top row: GP/UCSB. Middle row: UCSB/SDSU. Bottom row: SDSU/GP.